

STUDYING THE EFFECT OF PRODUCTIVE FACTORS ON SYNTHESIS OF NANOSTRUCTURE TiAl (γ) ALLOY BY MECHANICAL ALLOYING

F. Abbasi Nargesi*, R. Azari Khosroshahi and N. Parvini Ahmadi

Materials Engineering Faculty, Sahand University of Technology, P.O. Box 51335-1996 Tabriz, Iran
farshadabbasi60@yahoo.com , rakhosroshahi@sut.ac.ir , parvini@sut.ac.ir

*Corresponding Author

(Received: June 8, 2009 – Accepted in Revised Form: March 11, 2010)

Abstract In this research, the Planetary mill was used for mechanical alloying (MA) of Ti and Al powder mixture with equal at% ($Ti_{50}Al_{50}$). The effect of various factors, such as process control agent (PCA), speed of rotation of vial and ball-to-powder weight ratio, on process were studied and the best condition to synthesis the alloy was determined. Study on X-ray diffraction (XRD) patterns showed that at primary hours of milling, the powder mixture transmitted to metastable solid solution phase and with increasing the alloying time, that phase transformed to an amorphous, ultra fine grain and homogenous phase. Changes in grain size, lattice strain and impurity content during alloying and various condition were studied and at last with annealing of the product, the TiAl (γ) phase with high purity and nanostructured form was produced.

Keywords Titanium Aluminide, Nanostructure, Mechanical Alloying

چکیده در این تحقیق، آسیاب سیاره‌ای برای آلیاژسازی مکانیکی مخلوط پودری تیتانیوم و آلومینیوم با درصد اتمی یکسان ($Ti_{50}Al_{50}$) مورد استفاده قرار گرفت. اثر فاکتورهای مختلف، نظیر عامل کنترل‌کننده فرایند، سرعت چرخش محفظه آسیاب و نسبت گلوله به پودر بر روی فرایند مورد مطالعه قرار گرفت. و بهترین شرایط سنتز آن آلیاژ تعیین گردید. مطالعه بر روی الگوهای پراش اشعه ایکس نشان داد که در ساعتهای اولیه آسیاب، مخلوط پودری به فاز نیمه‌پایدار محلول جامد تبدیل شده و با افزایش زمان آلیاژسازی، آن فاز به فاز آمورف و هموزن و بسیار ریز تبدیل یافت. تغییرات در اندازه دانه، کرنش شبکه و میزان ناخالصی در طول آلیاژسازی و شرایط گوناگون مورد مطالعه قرار گرفت. در نهایت با آنیل نمودن محصول نهایی فرایند، فاز $TiAl(\gamma)$ با خلوص بالا و به شکل نانو ساختار حاصل گردید.

1. INTRODUCTION

Intermetallic compounds are the class of materials which possess many attractive properties for potential high-temperature applications. Titanium Aluminide intermetallics, particularly TiAl (γ) based alloys, have received a great deal of attention as candidate materials for high-temperature applications (aerospace and automobile industries), because of their low density, high specific strength, good oxidation and corrosion resistance at elevated temperatures [1-6].

A major disadvantage of TiAl alloys, however, is their poor room-temperature (RT) ductility. Such low RT ductility poses a major obstacle to the

widespread use of these materials, and recent studies and developments have focused on overcoming this problem [7-10].

Conventional casting of TiAl-base intermetallics is difficult due to their relatively high melting temperature and the extreme reactivity of titanium. More importantly, however, cast TiAl alloys are usually not suitable for subsequent forming as a result of inhomogeneities and segregation in the solidification microstructure combined with the lack of ductility [11, 12]. One possible approach to combine high strength with good RT ductility involves the use of ultra fine grain materials [12-14].

Mechanical alloying is a suitable method to

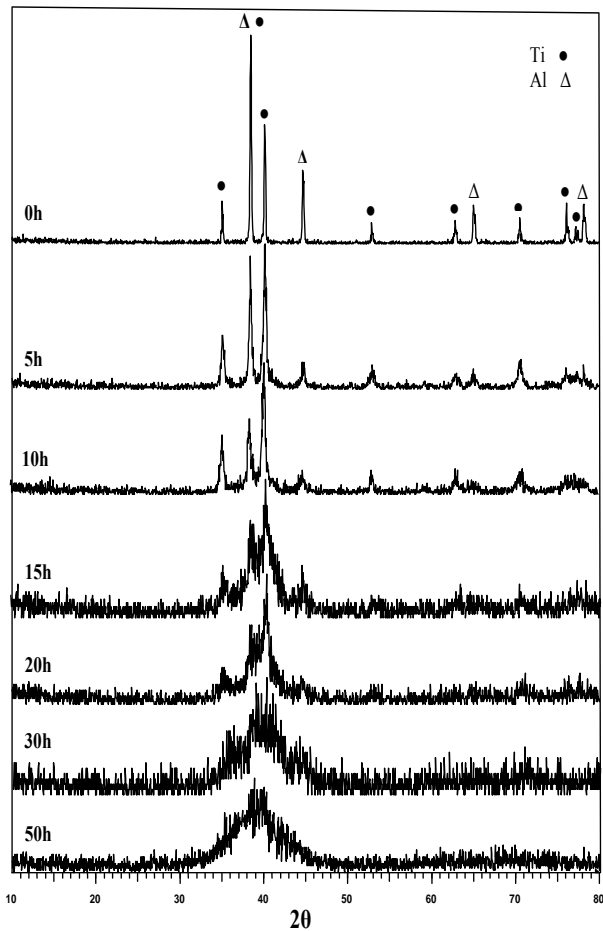


Figure 1. X-ray diffraction patterns of $Ti_{50}Al_{50}$ elemental powder, mechanically alloyed at several alloying times and with 2wt% Methanol.

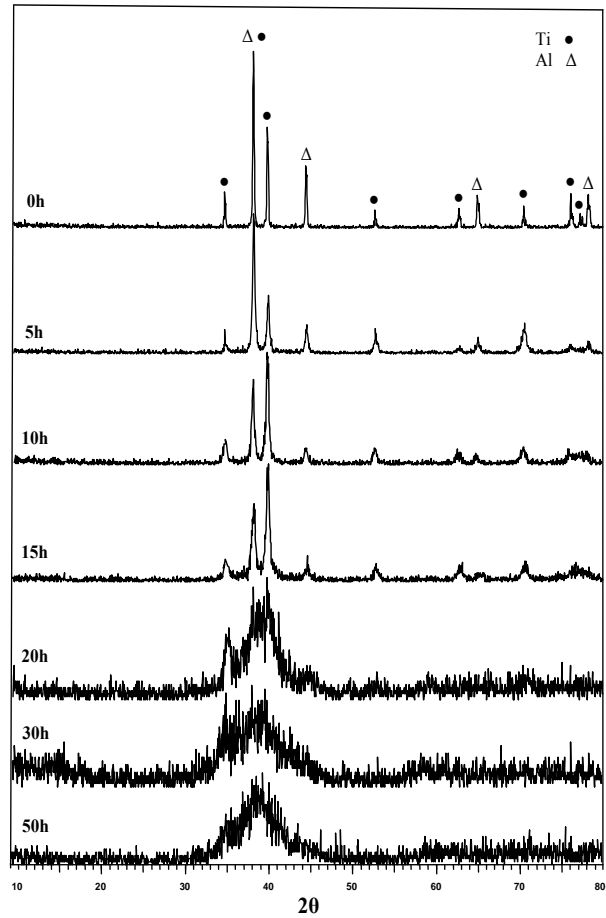


Figure 2. X-ray diffraction patterns of $Ti_{50}Al_{50}$ elemental powder, mechanically alloyed at several alloying times with 2wt% stearic acid.

produce TiAl (γ) intermetallic compounds in homogeneous and nano-scale form [14, 15].

During high-energy milling the particles are repeatedly flattened, cold welded, fractured and re-welded. True alloying among powder particles can occur only when a balance is maintained between cold welding and fracturing of particle [15-17].

In Mechanical alloying, a process control agent (PCA) is added to the powder mixture during milling to reduce the effect of cold welding. PCAs can be solids, liquids or gases. For example methanol, ethanol, stearic acid and ... are some PCAs. The PCA adsorbs on the surface of the powder particles and minimizes cold welding between powder particles and thereby inhibits agglomeration [18, 19].

2. EXPERIMENTAL PROCEDURE

The FP4 planetary mill with two tempered steel vials was employed in this research. The capacity of each vial was 250ml. Titanium of more than 99.7% purity and particle size 100-150 μ m and Aluminum of more than 99.5% purity and particle size ~100 μ m were used as starting powders. The initial weight of the powders to reach $Ti_{50}Al_{50}(\gamma)$ before MA was 10g and they were weighted in a glove box with argon atmosphere. Milling was conducted in tempered-steel vials with Cr-steel balls. The diameters of balls were 15, 20 mm. The vials were designed to allow pumping and subsequent filling by an inert gas (Ar) with high purity (near to 100% purity). The final gas pressure in the vial was kept to be 0.1MPa. The Two

different PCAs investigated in this study were methanol and stearic acid. Three ball-to-powder weight ratio (10:1, 15:1, 20:1) and two speed of rotation of supporting disk (450, 550 rpm) were used. The maximum alloying time accumulated was 50h. To avoid temperature increase during M.A, periods of 0.5h alternated with an equal rest time. After alloying time (5, 10, 15, 20, 30, 50h), the powders were withdrawn from the vials for analysis (X-ray diffraction measurement).

XRD measurements were performed by Bruker-D8-Advanced, using Cu-K α radiation at 30kv and 20mA. Analysis of the powder morphology and particle size measurements was achieved by Cam Scan MV-2300 SEM with EDS analyzer at an accelerating voltage of 25kV.

The crystallite size and lattice strain of the powder particles were determined using the X-ray peak broadening techniques (Scherrer and Williamson-Hall formulas):

$$d = \frac{0.9\lambda}{B \cos \theta}$$

$$B \cos \theta = \frac{0.9\lambda}{d} + \eta \sin \theta$$

Where d is the crystallite size, λ is the wavelength of the X-radiation used, B is the peak width at half the maximum intensity, θ is Bragg angle and η is the strain [20]. Some samples were examined after mechanical treatment by differential thermal analysis (DTA) L62 HDSC. This test was performed in argon atmosphere. Annealing of samples was executed by Alcatel CFA-222 vacuum furnace.

3. RESULTS AND DISCUSSION

3.1. Effect of the state of PCA on MA process of Ti₅₀Al₅₀

XRD patterns of Ti₅₀Al₅₀ powder, mechanically alloyed with 2%wt methanol and stearic acid for several alloying times are shown in Fig.1 and 2 respectively.

The XRD patterns showed that the diffraction intensities drastically decreased and broadened after 5h alloying time. The diffraction peaks

corresponding to the Al disappeared at an early time, indicating solution of Al in Ti lattice.

Diffusion of Al in Ti lattice is faster than that of Ti in Al lattice [21].

The lattice parameters of the α -Ti after MA for 10h with methanol are approximately $a=0.255\text{nm}$ and $c=0.467\text{nm}$, whereas those before MA are approximately $a=0.258\text{nm}$ and $c=0.470\text{nm}$, so that about 2%volume shrinkage has occurred due to the diffusion of Al into Ti lattice, which promotes of Ti(Al) solid solution.

In Fig. 1 after 10h alloying, the metastable solid solution of Al in Ti phase and a small amount of metastable solid solution of Ti in Al were formed.

When stearic acid was used as a PCA, that metastable phase formed after 15h alloying time.

In both cases, observation of shifts in the diffraction angles of Ti to higher angles indicated the formation of a solid solution of Al in Ti and shrinkage of lattice parameters of Ti [21, 22].

The diffraction peaks around $2\theta=40^\circ$ can not be separated after an alloying time of 30h.

The formation of an amorphous-like phase or very fine particles has been strongly enhanced with increasing of alloying time [21]. Amorphization during MA, was a result of increasing the free energy of system. The continuous decrease in grain size (and consequent increase in grain boundary area) and a lattice expansion would also contribute to the increase in free energy of the system [20]. In both cases, that phase was formed completely after 50h.

The rate of alloying process in samples with methanol was slightly faster than the samples with stearic acid at primary times of alloying. The nature of PCA, its characteristic and advantage of liquid state of methanol than solid state of stearic acid are the reasons of this change.

The grain size and lattice strain of productions of MA process as a function of alloying time for two PCA are shown in Fig 3 and 4 respectively. The lattice strain of powder particles was increased and grain size was decreased with increasing alloying time, because the impact energy of the balls exerted on powder particles increased with increasing the milling time further.

At early times of alloying, the decreasing rate of grain size was significant and according to Fig. 4,

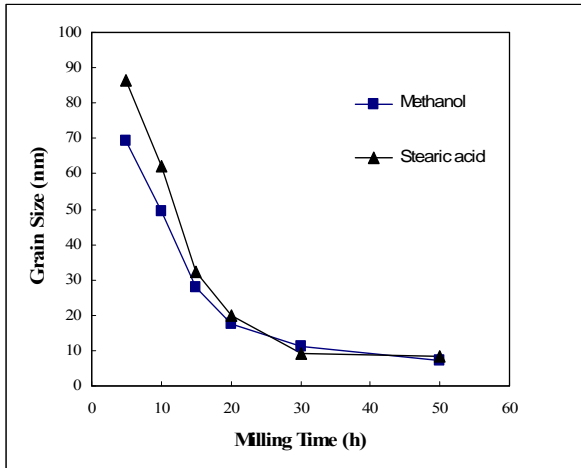


Figure 3. The average grain size of the M.A. powders as a function of alloying time for two PCA.

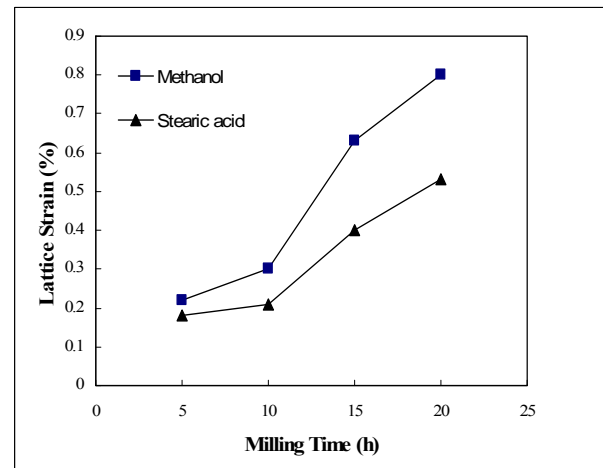


Figure 4. The lattice strain of productions of M.A process as a function of alloying time for two PCA.

after 15h milling, this rate decreased due to two factors, 1) small particles able to withstand extra deformation and 2) the balance achieved between the rate of welding and fracturing after specific alloying time.

Before 15h milling when methanol was used as a PCA, the decreasing rate of grain size was faster than stearic acid was used because methanol was liquid and more effective in decreasing the rate of fracturing at early alloying time.

Fig. 4 when stearic acid was used, the increasing rate of strain was less than when methanol was employed because methanol was more effective in decreasing the rate of cold welding at early time that caused distribution strain to more fractured particles. SEM images of mechanically alloyed $Ti_{50}Al_{50}$ powders at several alloying times with methanol and stearic acid are shown in Fig. 5 and 6, respectively.

These images indicate that methanol is more effective than stearic acid as a PCA at primary times of alloying. According to Fig. 5 and 6 at early time of milling, the stearic acid wasn't melted perfectly and the large particles were achieved that showed the domination of the rate of cold welding on fracturing at primary hours of milling, but in samples that included methanol, it was adsorbed on the surface of the particles easily and minimized cold welding. In this case, the rate

of fracturing dominated on cold welding at early hours of milling. In both cases, after alloying for certain length of time, a balance was achieved between the rate of welding and fracturing.

The weight recovered (g) as a function of alloying time for two PCA is shown in Fig.7.

When methanol was used as a PCA the weight recovered was reduced significantly after 10h alloying and with stearic acid this obvious reduction was after 15h alloying. Sticking tendency to milling tools caused this change. According to XRD patterns, it suggested when powder mixture transformed to Ti solid solution phase gradually, sticking tendency to milling tools were increased thus weight recovered was reduced.

3. 2. Effect of the Energy of Milling on MA process of $Ti_{50}Al_{50}$

The energy of milling can be increased by increasing the rotation speed of vial and ball-to-powder weight ratio (BPR). XRD patterns of $Ti_{50}Al_{50}$ powder, mechanically alloyed with 2%wt methanol and at 550rpm (rotation speed of vial) at several alloying times are shown in Fig. 8.

Increased milling energy (achieved by higher BPR, increased rotation speed of vial, etc.) is normally expected to introduce more strain and increase the defect concentration in the powder and thus lead to easier amorphization [20].

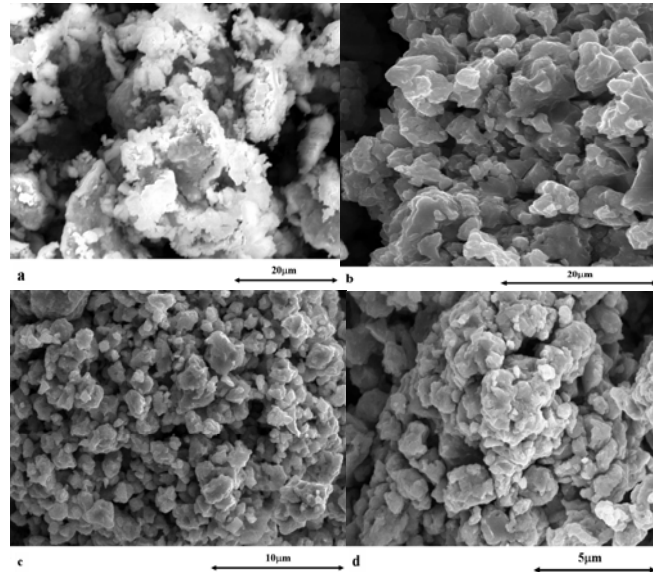


Figure 5. SEM micrographs of $Ti_{50}Al_{50}$ powders mechanically alloyed after (a) 5h, (b) 20h, (c) 30 and (d) 50h with 2%wt Methanol.

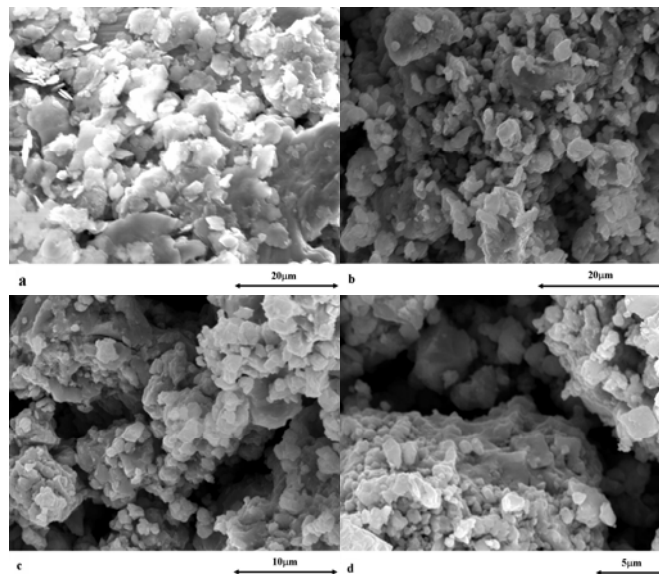


Figure 6. SEM micrographs of $Ti_{50}Al_{50}$ powders mechanically alloyed after (a) 5h, (b) 20h, (c) 30 and (d) 50h with 2%wt stearic acid.

In contrast to Fig. 1 (450rpm), when the vial rotated faster, the rate of the amorphization increased and a broadened peak achieved at the end of 20h milling with 550rpm that indicates an amorphous and ultra-fine grain production but at 450rpm that phase were produced after 30h milling. These changes occurred because the collision between balls-powder-vial increased at

higher speed and subsequently the defect concentration arose and ultra-fine grain powders achieved at shorter time.

SEM image of $Ti_{50}Al_{50}$ powder mechanically alloyed after 20h with 2%wt methanol and at 550rpm is shown in Fig. 9.

The higher rotation speed induced finer grain powders.

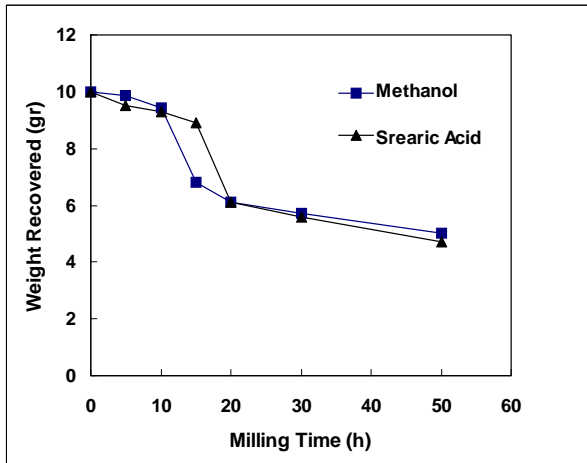


Figure 7. The weight recovered of production of process as a function of time for two PCA.

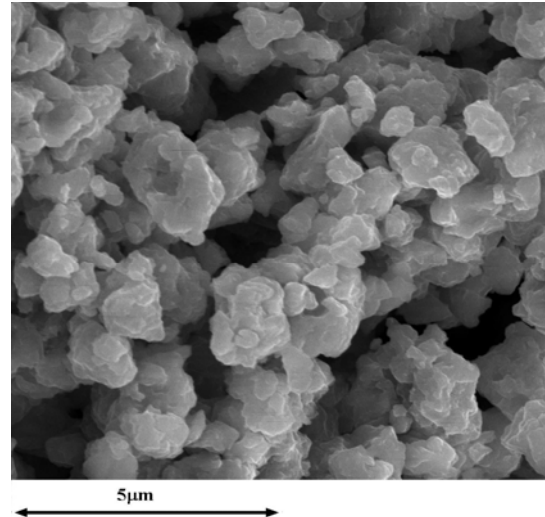


Figure 9. SEM micrographs of $Ti_{50}Al_{50}$ powders mechanically alloyed after 20h with 550 rpm.

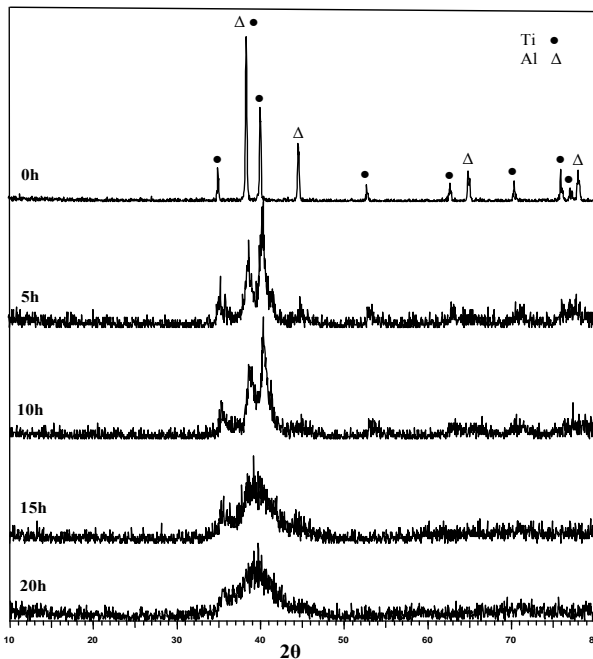


Figure 8. X-ray diffraction patterns of $Ti_{50}Al_{50}$ elemental powder, mechanically alloyed at several alloying times with 550rpm.

XRD patterns of the powder mixture mechanically alloyed with 2% methanol at 450rpm and 10:1, 20:1 BPR are shown in Fig. 10 and 11 respectively.

Regarding these figures, when ball-to-powder weight ratio was increased from 10:1 to 20:1, the amorphization and alloying process rate were increased because the content of balls and their weights increased and subsequently the energy of

the milling and collision arose. At 10:1 BPR, the metastable solid solution phase appeared after 15h and the amorphous phase wasn't produced after 30h milling but at 20:1 BPR the solid solution phase was resulted after 10h alloying time and the amorphous and fine grain phase was produced after 30h.

The Fe contamination as a function of milling time for two rotation speed of vial (450, 550 rpm) and two ball to powder weight ratio (10:1, 20:1) are shown in Fig. 12 and 13 respectively.

With increasing the milling energy, the collisions between balls and vial were increased thus the Fe contamination was increased in these cases.

The grain size and lattice strain of M.A products as a function of alloying time for two rotation speed and two BPR are shown in Fig. 14, 15 and 16 respectively.

The higher energy of milling caused finer grain size production and increased the lattice strain of the powder particles.

Finally with annealing the final product of alloying process (the sample mechanically alloyed for 50h at 450 rpm and 15:1 BPR) in vacuum oven for 10min at 900 °C, the $TiAl(\gamma)$ phase with high purity and 25nm average grain size was produced (Fig. 17, 18).

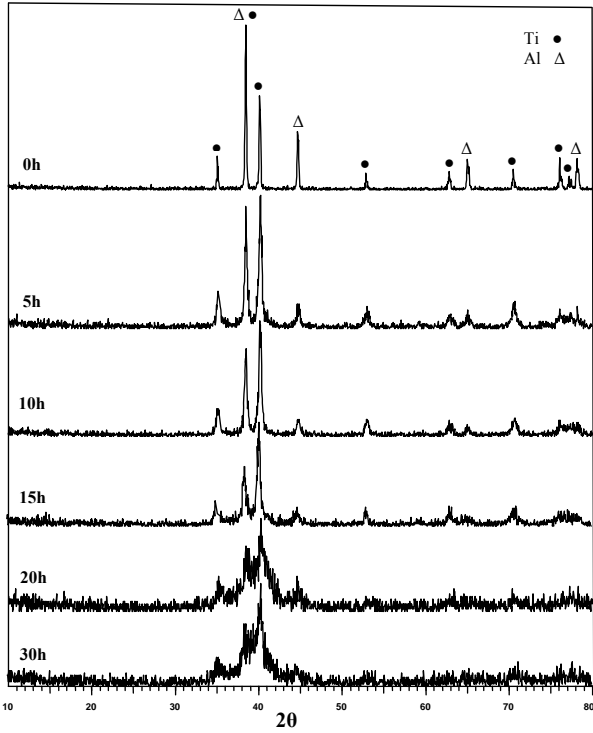


Figure 10. X-ray diffraction patterns of $Ti_{50}Al_{50}$ elemental powder, mechanically alloyed at several alloying times with 10:1 BPR .

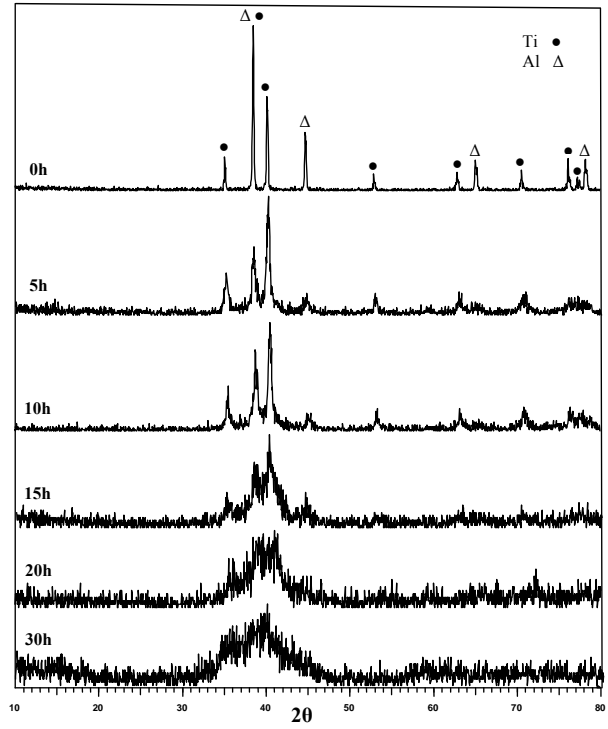


Figure 11. X-ray diffraction patterns of $Ti_{50}Al_{50}$ elemental powder, mechanically alloyed at several alloying times with 20:1 BPR .

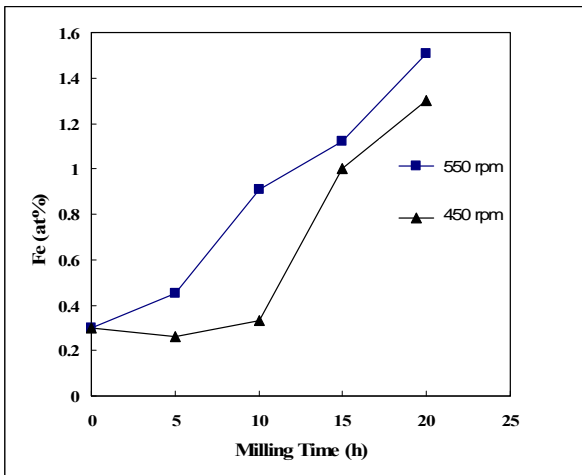


Figure 12. The Fe contamination (at %) of productions of M.A process as a function of alloying time for two rotation speed of vial.

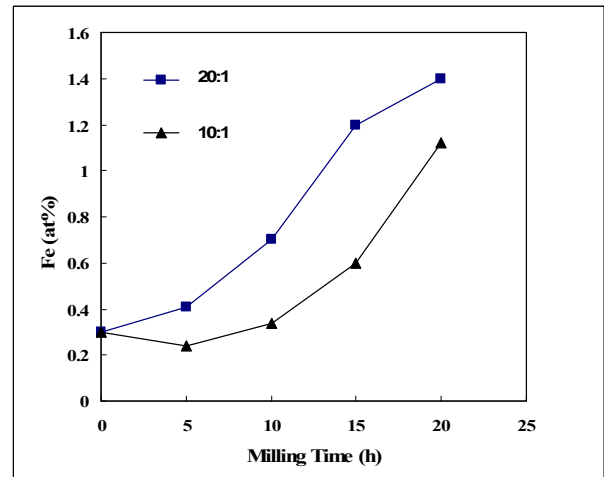


Figure 13. The Fe contamination (at%) of the product of M.A process as a function of alloying time for two BPR.

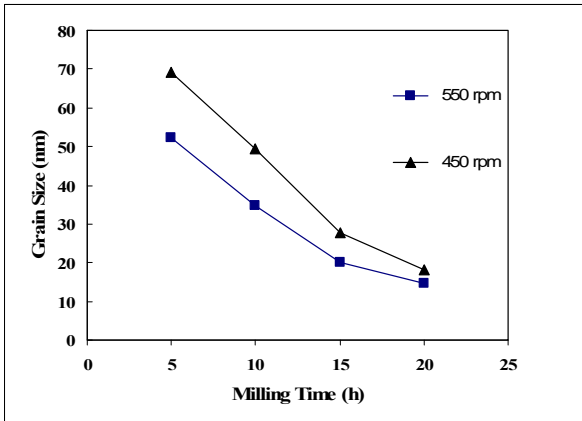


Figure 14. The average grain size of productions of M.A process as a function of alloying time for two rotation speed of vial (450, 550rpm).

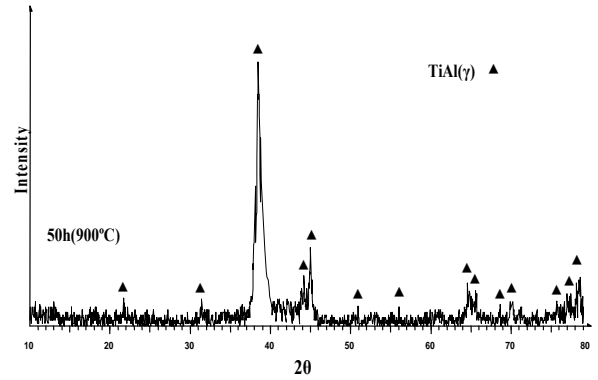


Figure 17. XRD pattern of mechanically alloyed $Ti_{50}Al_{50}$ after annealed at 900°C for 10min at vacuum furnace.

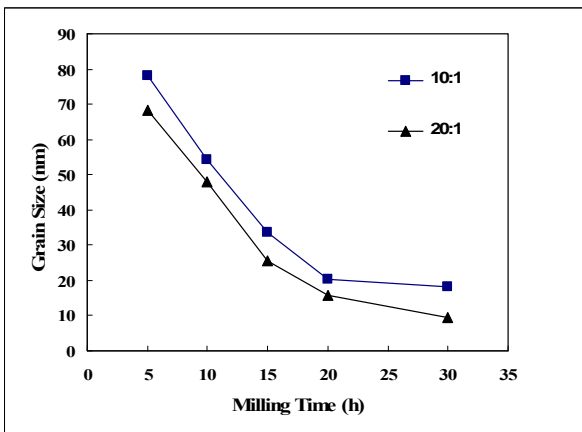


Figure 15. The average grain size of productions of MA process as a function of alloying time for two BPR (10:1, 20:1).

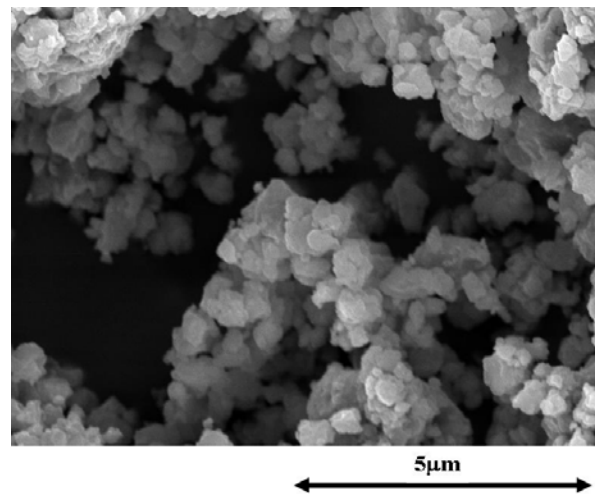


Figure 18. SEM micrographs of mechanically alloyed $Ti_{50}Al_{50}$ sample after annealing at 900 °C for 10min at vacuum oven.

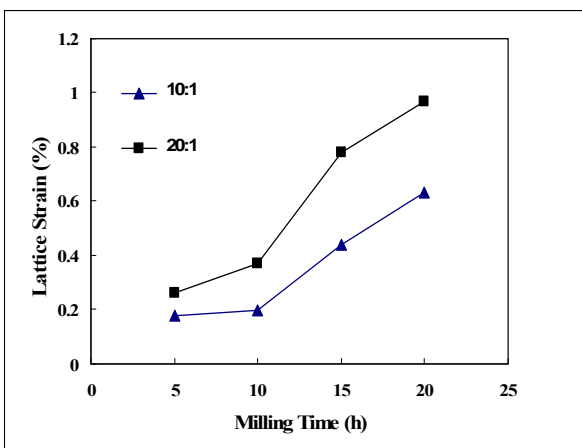


Figure 16. The lattice strain of productions of MA process as a function of alloying time for two BPR (10:1, 20:1).

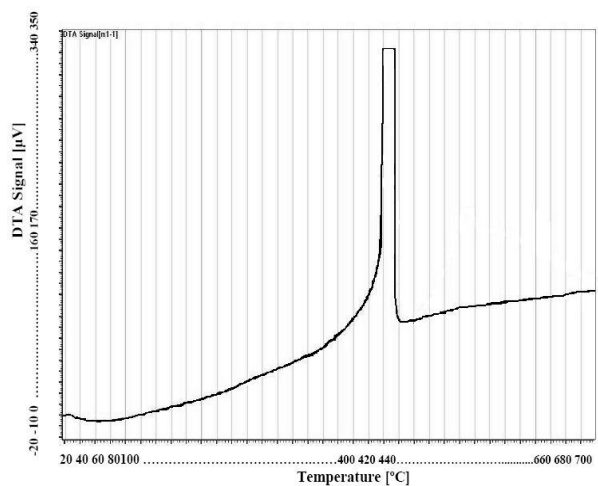


Figure 19. The curve of DTA test for 50h sample.

The result of DTA test on this sample showed an exothermic peak around 450 °C. This temperature represents the transformation of an amorphous TiAl to crystalline TiAl(γ) (Fig. 19).

4. CONCLUSION

- The Al diffraction peaks disappeared quickly during milling as a result of solution of Al in Ti lattice and formation of metastable solid solution Al in Ti phase.

- Increasing the alloying time accelerated the formation of the amorphous phase.

- When methanol was used as a PCA, the rate of alloying process was faster than when stearic acid was used at early alloying times, due to the nature of PCA, its characteristic and advantage of liquid state of methanol compared to the solid stearic acid.

- It was found that when Ti solid solution phase was produced gradually, the sticking tendency to milling tools increased thus the weight recovered reduced.

- Increasing the milling energy (by increased the rotation speed of vial and BPR) caused faster alloying process and amorphization rate.

- In higher milling energy, the grain sizes of productions were finer and strain lattice were increased because the impact energy and collision were higher in this condition.

- In higher milling energy, the Fe contamination content was increased.

- The TiAl(γ) phase produced after annealing process had high purity and ~25nm average grain size.

5. REFERENCES

1. E. Szewczak, J. Paszula, A. V. Lenov and H. Matyja, "Explosive Consolidation of Mechanically Alloyed Ti-Al Alloys", *Materials Science and Engineering A*, vol. 226, (1997), 115-117.
2. I. J. Polmer, "Light Alloys", Butterworth-Heineman Publication, (2006).
3. E. Hamzah, M. Kanniah, "Microstructure and Creep behaviour of as-cast Ti-48Al-4Cr", *Modern Applied Science*, vol. 3, (2009), 164-166.
4. Z. M. Sun, H. Hashimoto, "Fabrication of TiAl alloys by MA-PDS process and mechanical properties", *Intermetallics*, vol.11, (2003), 826-828.
5. S. C. Tjong, H. Chen, "Nanocrystalline Materials and Coatings", *Materials Science and Engineering R*, vol. 45, (2004), 14-36.
6. W. Maziarz, A. Michalski, "Structure and Mechanical Properties of Ball Milled Ti-Al-Cr Intermetallics Consolidated by Hot Pressing and Pulse Plasma Sintering", *Rev. Adv. Mater. Sci.*, vol. 8, (2004), 158-163.
7. P. Bhattacharya, P. Bellon, R. S. Averback, "Nanocrystalline TiAl Powder Synthesized by High-Energy Ball Milling: Effects of Milling Parameters on Yield and Contamination", *Journal of Alloys and Compounds*, vol. 368, (2004), 187-190.
8. K. Uenishi, T. Marsobara, "Nanostructured Titanium-Aluminides and Their Composites Formed by Combustion Synthesis of Mechanically Alloyed Powders", *Scripta Materialia*, vol. 44, (2001), 2094-2099.
9. K. B. Gerasimov, S. V. Pavlov, "Metastable Ti-Al Phases Obtained by Mechanical Alloying", *Journal of Alloys and Compounds*, vol. 242, (1996), 136-140.
10. S. H. Kim, H. H. Chung, "Effect of B on the Microstructure and Mechanical Properties of Mechanically Milled TiAl Alloys", *Metallurgical and Materials Transaction A*, vol. 20, (1998), 2273-2275.
11. E. Paransky, E. Y. Gutmanas, I. Gotman and M. Koczak, "Pressure Assisted Reactive Synthesis Of Titanium Aluminides From Dense 50Al-50Ti Elemental Powder Blends", *Metallurgical and Materials Transaction A*, vol. 27, (1996), 2130-2136.
12. F. H. Froes, C. Suryanarayana, K. Russel and C. G. Li, "Synthesis of Intermetallics by Mechanical Alloying", *Materials Science and Engineering A*, vol. 192, (1995), 612-623.
13. L. Lu, M. O. Lai and F. H. Froes, "The Mechanical Alloying of Titanium Aluminides", *JOM*, vol. 54, (2002), 62-64.
14. M. Sherif El-Eskandarany, "Mechanical Alloying for Fabrication of Advanced Engineering Materials", William Andrew Publication, USA, (2001).
15. C. Suryanarayana, "Recent Developments in Mechanical Alloying", *Rev. Adv. Mater. Sci.*, vol. 18, (2008), 203-211.
16. M. Bermudez, F. J. Carrion, P. Iglesias, "Influence of Milling Conditions on the Wear Resistance of Mechanically Alloyed Aluminum", *Wear*, vol. 258, (2005), 906-908.
17. J. R. Harris, J. D. Wattis, J. V. Wood, "A Comparison of Different Models for Mechanical Alloying", *Acta Mater.*, vol. 49, (2001), 3991-4000.
18. Y. F. Zhang, L. Lu and S. M. Yap, "Prediction of The Amount of PCA for Mechanical Milling", *Materials Processing Technology*, vol. 90, (1999), 260-267.
19. S. Kleiner, F. Bertocco, F. A. Khalid and O. Beffort, "Decomposition of Process Control Agent During Mechanical Milling and Its Influence On Displacement Reactions In The Al-TiO₂ System", *Materials Chemistry and Physics*, vol. 89, (2005), 362-366.

20. C. Suryanarayana, "Mechanical Alloying and Milling", *Progress in Materials Science*, vol. 46, (2001), 100-140.
21. L. Lu, M. O. Lai, "Mechanical Alloying", Kluwer Academic Publishers, Boston, (1998).
22. A. Takasaki, Y. Furuya, "Mechanical Alloying of The Ti-Al System in Atmosphere of Hydrogen and Argon", *Nanostructured Materials*, vol.11, (1999), 1209-1215.